

Effect of Structural Modification on the Catalytic Property of Mn-Substituted Hexaaluminates

MASATO MACHIDA, KOICHI EGUCHI, AND HIROMICHI ARAI

Department of Materials Science and Technology, Graduate School of Engineering Sciences, Kyushu University 39, 6-1 Kasugakoen, Kasuga, Fukuoka 816, Japan

Received October 25, 1989; revised January 19, 1990

The effects of structural modification on the catalytic properties of Mn-substituted hexaaluminates were investigated with a view toward developing a high-temperature combustion catalyst. The surface areas and catalytic activities of Mn-substituted hexaaluminates are significantly enhanced when the mirror plane cations are partially replaced by aliovalent cations of the same size. In the $\text{Sr}_{1-x}\text{La}_x\text{MnAl}_{11}\text{O}_{19-\alpha}$ system calcined at 1300°C, Sr substitution gave rise to the maximum surface area, 23.8 m²/g, and the maximum combustion activity ($T_{10\%} = 500^\circ\text{C}$) at $x = 0.2$. Transmission electron microscopy revealed that the substitution thinned the planar crystals of hexaaluminate and thus increased the surface area. Although the increase in catalytic activity corresponds to that in surface area, Sr substitution also affects the oxygen sorption property and the oxidation state of Mn ions in the hexaaluminate lattice. In particular, oxygen species desorbed at high temperatures (650–800°C) appear to play an important role in catalytic reaction. These oxygen species are related to the oxidation/reduction of Mn ion, which is brought into the highest oxidation state by the partial substitution. © 1990 Academic Press, Inc.

INTRODUCTION

Catalytic combustion has many advantages over conventional flame combustion in suppressing NO_x emission and in improving energy efficiency simultaneously (1–3). Although many industrial applications, such as gas turbines, boilers, and jet engines, are proposed, the most crucial subject is still how to develop heat-resistant catalyst materials. In particular, retention of a large surface area is one of the important factors used to evaluate the catalytic property.

We have investigated the heat resistance and catalytic properties of hexaaluminate-related compounds, which show outstanding heat resistance against sintering above 1300°C (4–6). The hexaaluminate structure comprises alternative stacks of Al–O spinel blocks and a monatomic layer (mirror plane) along the *c* axis as shown in Fig. 1. The hexaaluminate can be divided into two types of similar crystal structures, i.e., magnetoplumbite (Fig. 1) and β-alumina,

according to the ionic configuration in the mirror plane (7–9). A wide variety of large cations can occupy the site in the mirror plane as reported so far (10–12). It should be noted that the retention of large surface area is a common property of the hexaaluminate compounds, because the layered structure appears to play a key role in suppressing crystal growth along the *c* axis (13). Preparation from metal alkoxides further enhances the surface area to be above 10 m²/g after calcination at 1600°C (6). Such a heat-resistant ultrafine particle is quite useful as a high-temperature combustion catalyst operated above 1300°C (14).

In previous studies (15, 16), we reported microstructures and catalytic properties of cation-substituted hexaaluminates, BaM Al₁₁O_{19-α} (*M* = Cr, Mn, Fe, Co, and Ni). Among the series of catalysts, the Mn-substituted sample showed the highest activity for methane combustion because of the ease of the reduction/oxidation cycle of Mn-species in the hexaaluminate lattice. However, when the increase in Mn content

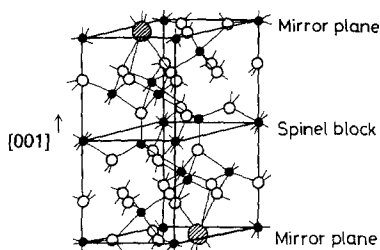


FIG. 1. Crystal structure of magnetoplumbite-type hexaaluminate: \odot , Large cation; \bullet , Al, Mn; \circ , oxygen.

leads to precipitation of other phases, the surface area and catalytic activity of this system are lowered significantly. Thus, to enhance the catalytic activity of Mn-substituted hexaaluminate without increasing Mn content, other structural modifications are necessary.

In this study, we investigated the effect of partial substitution of cations in the mirror plane on the catalytic properties of Mn-substituted hexaaluminates. Emphasis has been placed on elucidating the effect of partial substitution of the mirror plane cation on catalytic activity and surface area.

EXPERIMENTAL

Catalyst Preparation

Manganese-substituted hexaaluminates, $A_{1-x}A'_xMnAl_{11}O_{19-\alpha}$ ($A = Ba, Sr, Ca, La, K$; $A' = Sr, La, K, Ca$) were prepared by hydrolysis of metal alkoxides. Corresponding metal isopropoxides or ethoxides were dissolved in 2-propanol and kept at 80°C for 5 h. After an aqueous solution of manganese nitrate was added to the alcoholic solution, the precipitate thus formed with gelation was evaporated to dryness. All samples were calcined at 1300°C prior to use in the catalytic reaction. Crystal structures of calcined samples were determined by X-ray diffraction (Rigaku Denki, 4011) with $CuK\alpha$ radiation. Specific surface areas of calcined samples were measured by the BET method using nitrogen adsorption.

Transmission Electron Microscopy (TEM)

A transmission electron microscope (JEOL, JEM-2000FX) was used for studying crystal morphology, crystal orientation, and crystal size distribution. Selected-area electron diffraction (SAD) was applied for determining the crystal orientation. The crystal size was obtained when the incident electron beam was parallel or normal to the c axis of the hexaaluminate. One hundred crystallites were used to obtain the crystal size distribution.

Catalytic Combustion of Methane

Catalytic activities were measured in a conventional flow system at atmospheric pressure. Catalysts were fixed in a quartz reactor by packing alumina beads at both ends of the catalyst bed. A gaseous mixture of methane (1 vol%) and air (99 vol%) was fed to the catalyst bed at a flow rate of 48,000 $cm^3 h^{-1}$ (space velocity = 48,000 h^{-1}). The methane conversion in the effluent gas was analyzed by on-line gas chromatography. In this study, the combustion activity is expressed as temperatures, $T_{10\%}$, at which the conversion is 10%, to neglect the effect of a mass transfer process and a gas-phase reaction.

Temperature Programmed Desorption of Oxygen

Temperature programmed desorption (TPD) of oxygen was measured in a flow system. Prior to the measurement, the sample was treated in an oxygen stream (50 ml/min) at 800°C for 1 h; this was followed by cooling to room temperature. After evacuation, the sample was heated at a constant rate of 10°C/min in a He stream (50 ml/min). The desorbed oxygen in the effluent gas was detected with a TCD cell.

Thermogravimetry

The oxidation state of Mn ions was determined with a thermogravimeter (Shimadzu DT-40) equipped with a flow system. Prior to measurement, the sample was heated at

1000°C in a stream of dry air to remove physisorbed water and then cooled to room temperature. After evacuation, the sample was heated again at the constant rate of 10°C/min in a H₂ stream (30 ml/min). The decrease in sample weight corresponding to the degree of reduction was recorded up to 1100°C. The oxidation state of Mn ions was calculated from the weight loss as mentioned in the previous paper (9).

RESULTS

Effect of Cation Compositions in the Mirror Plane of Mn-Substituted Hexaaluminates

Crystalline phases, surface areas, and catalytic activities of Mn-substituted hexaaluminates with various mirror plane cations are summarized in Table 1. In this study, alkaline earth (Ba, Sr, and Ca), alkaline (K), rare earth (La), and their composite metal elements were selected as the mirror plane cations. The crystal structures of both BaMnAl₁₁O_{19-α} and BaAl₁₂O₁₉ are of the hexaaluminate type (10), whereas SrMnAl₁₁O_{19-α} appears to be a mixture of two hexaaluminate phases as described be-

low. The hexaaluminate structure is also retained for LaMnAl₁₁O_{19-α}. These three samples, composed of hexaaluminate phases, possessed large surface areas (ca. 13 m²/g) similarly to unsubstituted hexaaluminates. However, the CaMnAl₁₁O_{19-α} sample decomposed into CaAl₁₂O₁₉ and CaAl₄O₇ phases. Precipitation of the second phase lowered the surface area and the catalytic activity due to significant sintering during calcination.

Substituents A' in A_{0.8}A'_{0.2}MnAl₁₁O_{19-α} are chosen with attention to the deviation of the ionic radius and valence from those of the host cation. Thus, the ratio of the ionic radii of A and A', r_M, is defined as shown in Table 1. The three types of combination of large cations in the mirror plane were examined for partial substitution, i.e., (1) same valent cations, (2) aliovalent and different-size cations, (3) aliovalent and same-size cations. Potassium cations occupied the Ba site without any phase separation after calcination at 1300°C. Both surface area and catalytic activity were strongly enhanced by substitution of K for Ba. Catalytic activity was also enhanced by Sr substitution for La (Sr_{0.8}La_{0.2}MnAl₁₁O_{19-α}) in which a single hexaaluminate phase attained a surface area of 23.8 m²/g. Other combinations of mirror plane cations were not effective in improving surface area and catalytic activity. It is noted that the substitution of mirror plane cations enhances the catalytic properties only when the size of an aliovalent substituent is close to that of the host cation or (r_M ≈ 1).

TABLE 1

Phases, Surface Areas, and Catalytic Activities of Mn-Substituted Hexaaluminates with Various Cation Compositions in the Mirror Plane

Composition	r _M ^a	Surface area (m ² g ⁻¹)	Catalytic activity, T _{10%} ^b (°C)	Crystalline phase
BaMnAl ₁₁ O _{19-α}	—	13.7	540	BA ₆
Ba _{0.8} K _{0.2} MnAl ₁₁ O _{19-α}	0.98	23.3	505	BA ₆
Ba _{0.8} La _{0.2} MnAl ₁₁ O _{19-α}	0.84	12.0	550	BA ₆ + α
Ba _{0.8} Sr _{0.2} MnAl ₁₁ O _{19-α}	0.85	15.1	535	BA ₆
SrMnAl ₁₁ O _{19-α}	—	13.4	540	Quasi-SA ₆
Sr _{0.8} La _{0.2} MnAl ₁₁ O _{19-α}	0.98	23.8	500	SA ₆
Sr _{0.8} K _{0.2} MnAl ₁₁ O _{19-α}	0.87	12.9	550	Quasi-SA ₆
Sr _{0.8} Ca _{0.2} MnAl ₁₁ O _{19-α}	0.86	7.3	550	Quasi-SA ₆
CaMnAl ₁₁ O _{19-α}	—	4.0	565	CA ₆ + CA ₂

Note. All samples were calcined at 1300°C for 5 h.

^a Ratio of ionic radii A and A' of A_{0.8}A'_{0.2}MnAl₁₁O_{19-α}.

^b Temperature at which conversion level is 10%. Reaction conditions: CH₄, 1 vol%; air, 99 vol%; S.V., 48,000 h⁻¹.

^c BA₆ = BaAl₁₂O₁₉, SA₆ = SrAl₁₂O₁₉, CA₆ = CaAl₁₂O₁₉, CA₂ = CaAl₄O₇, α = α-Al₂O₃.

Crystal Structure, Surface Area, and Catalytic Activity of Sr_{1-x}La_xMnAl₁₁O_{19-α}

It became evident that the Ba_{0.8}K_{0.2}MnAl₁₁O_{19-α} and Sr_{0.8}La_{0.2}MnAl₁₁O_{19-α} samples showed the prominent features of a combustion catalyst, but volatilization of potassium excludes the use of K-containing samples at high temperatures. Thus, further investigation was focused on the Sr_{1-x}La_xMnAl₁₁O_{19-α} system, in which

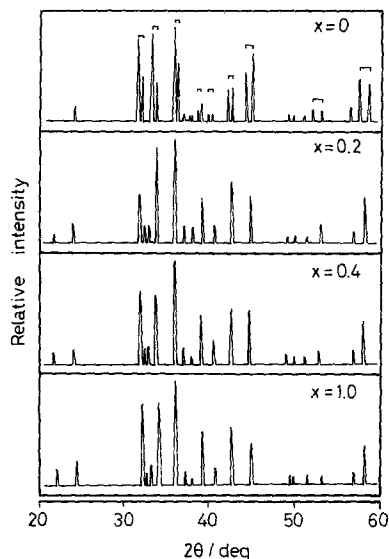


FIG. 2. X-ray diffraction patterns of $\text{Sr}_{1-x}\text{La}_x\text{MnAl}_{11}\text{O}_{19-\alpha}$ after calcination at 1300°C .

large surface area and high catalytic activity are simultaneously attained.

The crystal structure of $\text{Sr}_{1-x}\text{La}_x\text{MnAl}_{11}\text{O}_{19-\alpha}$ was studied by X-ray diffraction after calcination at 1300°C (Fig. 2). The samples consisted of the two hexaaluminate phases at $0 < x < 0.1$. Analytical electron microscopic analysis indicated that one of these hexaaluminate phases contains more Mn ions than the other. The diffraction peaks ascribable to the hexaaluminate of low Mn content were diminished by the substitution of Sr for La. Finally, a single

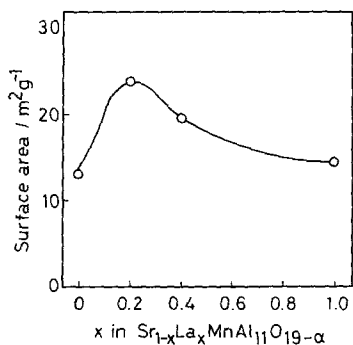


FIG. 3. Surface areas of $\text{Sr}_{1-x}\text{La}_x\text{MnAl}_{11}\text{O}_{19-\alpha}$ after calcination at 1300°C .

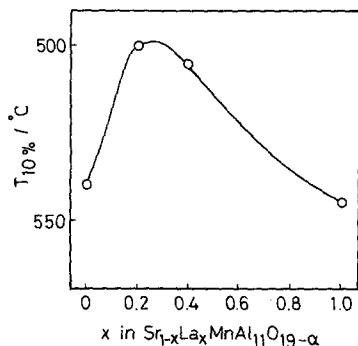


FIG. 4. Catalytic activity of $\text{Sr}_{1-x}\text{La}_x\text{MnAl}_{11}\text{O}_{19-\alpha}$ for combustion of methane. $T_{10\%}$ = temperature at which CH_4 conversion is 10%. Reaction conditions: CH_4 , 1 vol%; air, 99 vol%; S.V., $48,000 \text{ h}^{-1}$.

hexaaluminate phase was obtained in the range $0.2 < x < 1.0$.

The surface areas of the samples after calcination at 1300°C are plotted as a function of x in Fig. 3. It is clearly shown that surface area increases with Sr substitution for La up to a maximum value of $23.8 \text{ m}^2/\text{g}$ at $x = 0.2$, but further substitution decreases surface area at $x > 0.2$.

Figure 4 shows the catalytic activities for methane combustion over $\text{Sr}_{1-x}\text{La}_x\text{MnAl}_{11}\text{O}_{19-\alpha}$. The ignition temperature ($T_{10\%}$) of the system decreased with increasing x and maximum activities were obtained at $x = 0.2$, at which the surface area is at a maximum, as shown in Fig. 3. The relative oxidation activities of $\text{Sr}_{1-x}\text{La}_x\text{MnAl}_{11}\text{O}_{19-\alpha}$ are summarized in Table 2 as reaction rates

TABLE 2

Relative Reaction Rate of CH_4 Combustion Over $\text{Sr}_{1-x}\text{La}_x\text{MnAl}_{11}\text{O}_{19-\alpha}$

x	Reaction rate at 500°C	
	Per unit mass ($\text{mmol g}^{-1} \text{ min}^{-1}$)	Per unit surface area ($\text{mmol m}^{-2} \text{ min}^{-1}$)
0	1.72	1.28
0.2	4.79	2.01
0.4	3.66	1.83
1.0	0.38	0.25

per unit mass and per unit surface area. The activity per unit mass corresponds well to the increase in surface area, being maximum at $x = 0.2$. When the activity is obtained per unit surface area, the effect of substitution is depressed, e.g., the activity ratio at $x = 0$ to $x = 0.2$ is 2.8 per unit mass and is 1.6 per unit surface area. However, the relative activity at $x = 0.2$ is still a magnitude higher than at $x = 1.0$. This means that the increase in catalytic activity resulted from not only the surface area but also the net activity of the unit catalyst surface.

Crystal Morphology and Crystal Size Distribution

Transmission electron microscopy revealed that the sample crystallizes as hexagonal planar particles about 20 nm thick, which is one-fifth to one-tenth their diameters (Fig. 5). The planar morphology of the hexaaluminate crystal reflects well the lay-

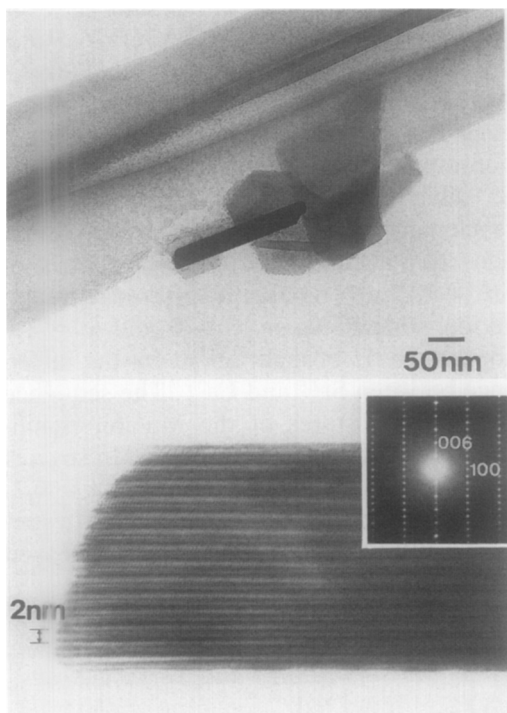


FIG. 5. TEM photographs of $\text{LaMnAl}_{11}\text{O}_{19-\alpha}$ after calcination at 1300°C .

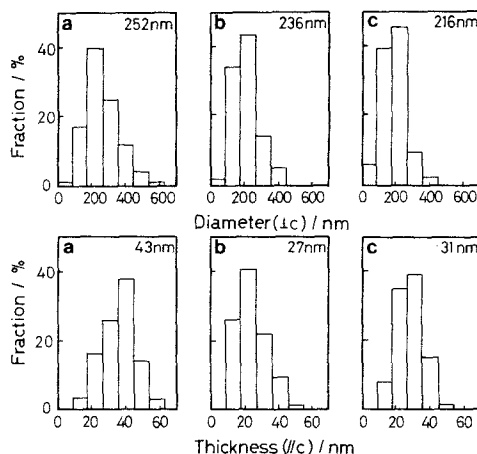


FIG. 6. Crystal size distributions of $\text{Sr}_{1-x}\text{La}_x\text{MnAl}_{11}\text{O}_{19-\alpha}$ after calcination at 1300°C . (a) $x = 0$, (b) $x = 0.2$, (c) $x = 1.0$. Numbers show the averages.

ered structure. The flat facet orientation is normal to the c axis as revealed by electron diffraction. A high-resolution image with an incident beam normal to the (110) plane showed the evidence of an array of spinel layers along the c axis. From this anisotropic shape of crystallites, the crystal growth of hexaaluminate along the c axis is expected to be strongly suppressed in this system. Since this crystal habit was observed in all the samples, anisotropic crystal growth may be the reason the large surface area is retained.

To elucidate the change in surface area of $\text{Sr}_{1-x}\text{La}_x\text{MnAl}_{11}\text{O}_{19-\alpha}$, the distribution of the diameter and the thickness of the planar crystallites was obtained for samples at $x = 0, 0.2,$ and 1.0 (Fig. 6). For each sample, the peak in the diameter distribution is situated at around 200 nm, and the average diameter decreased gradually with increasing x . On the other hand, the thickness of the partially substituted sample (27 nm at $x = 0.2$) is small compared with those of the terminal compositions (43 nm at $x = 0, 31$ nm at $x = 1.0$). This shows that the increase in surface area apparently results from the decrease in thickness of the hexagonal facet.

Temperature Programmed Desorption of Oxygen

To elucidate the catalytic activity of $\text{Sr}_{1-x}\text{La}_x\text{MnAl}_{11}\text{O}_{19-\alpha}$, TPD of oxygen was measured after treatment in an O_2 flow at 1000°C . The TPD curves thus obtained are shown in Fig. 7 as a function of temperature. $\text{Sr}_{1-x}\text{La}_x\text{MnAl}_{11}\text{O}_{19-\alpha}$ samples showed two desorption peaks, i.e., one below 400°C and the other above 700°C . La substitution reduced the amount of desorption at low temperatures and enhanced the amount of desorption at temperatures up to the maximum at $x = 0.2-0.4$, at which the highest catalytic activity was obtained. Total oxygen desorption at $x = 0$ is about 0.1 mmol/g and it decreased monotonously with Sr substitution. The two kinds of oxygen desorption differ in their reversibility. Treatment of the sample in an O_2 flow at 1000°C after TPD measurement restored only the high-temperature peaks. This means that the desorption occurred reversibly only for the oxygen species desorbed at high temperatures. The catalytic activity of $\text{Sr}_{1-x}\text{La}_x\text{MnAl}_{11}\text{O}_{19-\alpha}$ appears to be associated with high-temperature oxygen desorption.

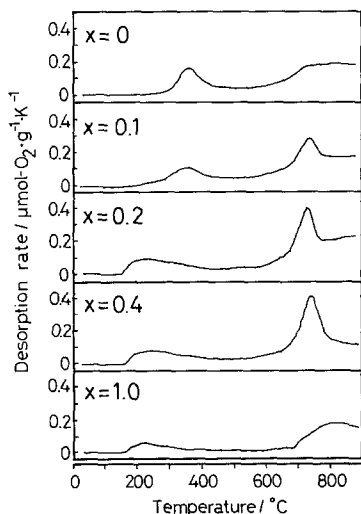


FIG. 7. TPD profiles of oxygen from $\text{Sr}_{1-x}\text{La}_x\text{MnAl}_{11}\text{O}_{19-\alpha}$.

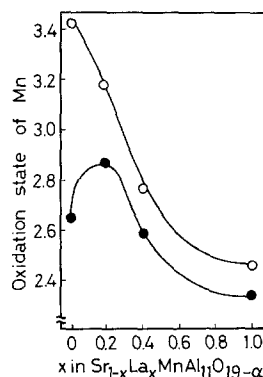


FIG. 8. Average oxidation state of Mn in $\text{Sr}_{1-x}\text{La}_x\text{MnAl}_{11}\text{O}_{19-\alpha}$. ○, Oxidation state at room temperature; ●, oxidation state at 300°C .

Oxidation State of Mn in $\text{Sr}_{1-x}\text{La}_x\text{MnAl}_{11}\text{O}_{19-\alpha}$

Since all the Mn species are reduced into divalent states after being heated in a H_2 flow up to 1000°C , the oxidation states of Mn ions in the hexaaluminate lattice can be determined from the weight loss accompanied by the reduction. The results thus obtained are shown in Fig. 8 as average oxidation states at room temperature and 300°C . At room temperature, the Mn species were in an oxidation state higher than $3+$. Oxidation number decreased monotonously with Sr substitution to 2.45 at $x = 1.0$. This result can be expected because charge compensation accompanies the replacement of Sr^{2+} with La^{3+} . Thus, the difference in oxidation state between $x = 0$ and $x = 1.0$ appears to be brought about by the difference between Sr^{2+} and La^{3+} . The sequence of oxidation states of the Mn ion significantly changed at 300°C and the Mn species is at the highest oxidation state at $x = 0.2$. The difference in oxidation state of Mn species in $\text{Sr}_{1-x}\text{La}_x\text{MnAl}_{11}\text{O}_{19-\alpha}$ decreased with increasing temperature.

DISCUSSION

Effect on Crystal Size and Surface Area

In this study, three kinds of combination of large cations in the mirror plane were examined for partial substitution in the

hexaaluminate catalyst. In the combinations of (1) same valent cations and (2) aliovalent and different-size cations, no effects were observed despite the single hexaaluminate formed. The structural modification appears to be effective only when the cations in the mirror plane are replaced by aliovalent cations of the same size.

TEM observation showed that the crystal morphology of the hexaaluminates is reflected in its layered structure. The hexagonal facet parallel to the (001) plane is caused by anisotropic crystal growth in which the successive formation of oxygen close-packed spinel blocks easily proceeds along the (001) plane. In crystal growth along the [001] direction, on the other hand, alternative stacking of a spinel block and a monatomic mirror plane appears to be a rather slower step. This is also deduced from the fact that each spinel block is weakly held together because they are individually partitioned by a monatomic mirror plane along the *c* axis (Fig. 1).

The increase in surface area of the $\text{Sr}_{1-x}\text{La}_x\text{MnAl}_{11}\text{O}_{19-\alpha}$ system is also related to the anisotropic crystal growth of the hexaaluminate. Since the same effect was observed in the samples without Mn species ($\text{Sr}_{1-x}\text{La}_x\text{Al}_{12}\text{O}_{19-\alpha}$), the change in surface area is ascribed to only the feature of the host crystal. It has become evident that the surface areas of $\text{Sr}_{1-x}\text{La}_x\text{MnAl}_{11}\text{O}_{19-\alpha}$ correspond to the thickness of the hexagonal facet as shown in Fig. 6. The increase in surface area resulted from the anisotropic crystal growth which is suppressed along the [001] direction. On the contrary, the diameter of the hexagonal facet depends less on the cation composition in the mirror plane. These results show that the stacking of a spinel block and a monatomic mirror plane appears to be greatly suppressed by the partial substitution of La for Sr.

Effect on Catalytic Activity

In Mn-substituted hexaaluminates, partial substitution of large cations in the mir-

ror plane enhances catalytic activity only when the large surface area was obtained. This means that surface area is one of the factors responsible for enhancement of activity in catalytic combustion. In fact, the specific activity per unit surface of the hexaaluminate catalyst is relatively low as reported previously (16). A large surface area is necessary to bring about sufficient combustion activity of the hexaaluminate catalysts. However, catalytic activity cannot be accounted for only by the surface area as in the case of $\text{Sr}_{0.8}\text{La}_{0.2}\text{MnAl}_{11}\text{O}_{19-\alpha}$. Table 2 shows that the activity per unit surface area of the catalyst increased with La substitution. Since the content of Mn ions is constant and, in addition, they disperse highly and homogeneously in the hexaaluminate lattice, the increase in catalytic activity should be ascribed to the net activity of the catalyst surface. This can be explained by the consistency between catalytic activity and oxygen desorption at high temperatures observed in TPD profiles.

Figure 9 shows the amounts of oxygen desorption for $\text{Sr}_{1-x}\text{La}_x\text{MnAl}_{11}\text{O}_{19-\alpha}$ in the entire temperature range (room temperature–900°C) and in the high-temperature peaks (650–800°C). The total amount of desorption decreased with increasing *x*. When only the high-temperature desorption peaks are noted, however, the amount of desorp-

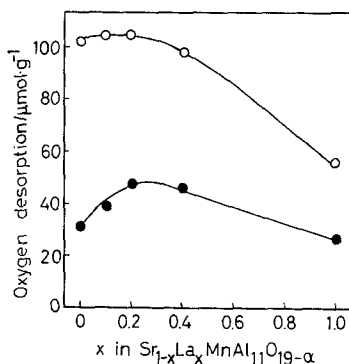


FIG. 9. Oxygen desorption from $\text{Sr}_{1-x}\text{La}_x\text{MnAl}_{11}\text{O}_{19-\alpha}$. ○, Total desorption (room temperature–900°C); ●, high-temperature desorption (650–800°C).

tion reaches the maximum at $x = 0.2$. The difference between the two curves in Fig. 9 results from the low-temperature oxygen desorption, which becomes dominant especially at lower x values (Fig. 7).

As mentioned in the previous report (16), oxygen sorption and desorption on the hexaaluminate accompany the reduction/oxidation of Mn species in the lattice. In the $\text{Sr}_{1-x}\text{La}_x\text{MnAl}_{11}\text{O}_{19-\alpha}$ system, it can be also recognized that oxygen desorption and the oxidation states of Mn ions are closely related from the rough comparison between Figs. 8 and 9. Thermogravimetric analysis showed that the average oxidation state of the Mn ion at room temperature is reduced by Sr substitution from 3.4 to 2.4. The charge compensation through Sr substitution appears to reduce the oxidation state of Mn ions and accordingly the total amount of desorption of oxygen. In addition, in the sample which shows large desorption at low temperature ($<400^\circ\text{C}$), the oxidation state of Mn species was significantly reduced by heating at 300°C , resulting in a maximum at $x = 0.2$. Thus, most low-temperature desorption corresponds to the difference in oxidation state of Mn at room temperature and at 300°C . The oxygen species desorbed at low temperatures were easily desorbed from catalysts, but the reverse process is too slow to contribute to catalytic oxidation, probably due to the instability of the high oxidation state of Mn.

On the other hand, the oxygen species desorbed at high temperatures showed good reversibility in the TPD measurement. These results indicate that the oxygen species, which desorb at high temperatures, play an important role in catalytic reaction. This is why catalytic combustion of methane begins at about 500°C at which the high-temperature peak appeared. Since the average oxidation number is less than 3.0 above 300°C (Fig. 8), the possible reduction/oxidation couple, which contributes to the high-temperature desorption of oxygen, is $\text{Mn}^{2+}-\text{Mn}^{3+}$. In fact, the spectroscopic anal-

ysis by Laville *et al.* (17) showed that Mn species are in mixed oxidation states of 2+ and 3+ in the La hexaaluminate.

Sr substitution reduces the total oxidation states of Mn ions, but maintains the high oxidation state at reaction temperatures. The catalytic activity of $\text{Sr}_{1-x}\text{La}_x\text{MnAl}_{11}\text{O}_{19-\alpha}$ is enhanced by the oxygen desorption which is caused by the high oxidation state of Mn ion thus produced by Sr substitution in the hexaaluminate lattice.

CONCLUSION

The present study has demonstrated that the catalytic activities and surface areas of Mn-substituted hexaaluminates are simultaneously enhanced by the structural modification in the mirror plane. In particular, partial substitution of Sr for La attained the large surface area ($23.8 \text{ m}^2/\text{g}$) and the low ignition temperature ($T_{10\%} = 500^\circ\text{C}$) after calcination at 1300°C . Such superior heat resistance is quite useful for a high-temperature combustion catalyst. The effect of structural modification appears to be ascribed to (1) the suppression of crystal growth along the c axis which enhances the surface area and (2) the increase in oxidation number of Mn ions which promotes active oxygen desorption.

ACKNOWLEDGMENT

Electron microscopic experiments in this study were carried out in the High Voltage Electron Microscopy Laboratory of Kyushu University.

REFERENCES

1. Trimm, D. L., *App. Catal.* **7**, 249 (1984).
2. Prasad, R., Kennedy, L. A., and Ruckenstein, E., *Catal. Rev.* **26**, 1 (1984).
3. Pfefferle, L. D., and Pfefferle, W. C., *Catal. Rev.* **29**, 219 (1987).
4. Machida, M., Eguchi, K., and Arai, H., *Chem. Lett.*, 767 (1987).
5. Machida, M., Eguchi, K., and Arai, H., *J. Catal.* **103**, 385 (1987).
6. Machida, M., Eguchi, K., and Arai, H., *Bull. Chem. Soc. Japan* **61**, 3659 (1988).
7. Steevens, A. L. N., and Schrama-de Pauw, A. D. M., *J. Electrochem. Soc.* **125**, 691 (1976).

8. Steevens, A. L. N., and Verstegen, J. M. P. J., *J. Lumin.* **14**, 207 (1976).
9. Verstegen, J. M. P. J., and Steevens, A. L. N., *J. Lumin.* **9**, 406 (1974).
10. Saber, D., and Lejus, A. M., *Mater. Res. Bull.* **16**, 1325 (1981).
11. Laville, F., and Lejus, A. M., *J. Cryst. Growth* **63**, 426 (1983).
12. Iyi, N., Takekawa, S., and Kimura, S., *J. Solid State Chem.* **83**, 8 (1989).
13. Machida, M., Kawasaki, H., Eguchi, K., and Arai, H., *Nippon Kagaku Kaishi*, 2010 (1988).
14. Machida, M., Eguchi, K., and Arai, H., *J. Amer. Ceram. Soc.* **71**, 1142 (1988).
15. Machida, M., Eguchi, K., and Arai, H., *Chem. Lett.*, 767 (1987).
16. Machida, M., Eguchi, K., and Arai, H., *J. Catal.* **120**, 377 (1989).
17. Laville, F., Gourier, D., Lejus, A. M., and Vivien, D., *J. Solid State Chem.* **49**, 180 (1983).